

MONOTONIC AND CYCLIC BEHAVIOUR OF TRABECULAR BONE
UNDER UNIAXIAL AND MULTIAXIAL LOADING

MOHD AL-FATIHHI BIN MOHD SZALI JANUDDI

A thesis submitted in fulfilment of the
requirements for the award of the degree of
Doctor of Philosophy (Mechanical Engineering)

Faculty of Mechanical Engineering
Universiti Teknologi Malaysia

DECEMBER 2015

To my beloved parents, wife, and daughter

ACKNOWLEDGEMENT

In the name of Allah, the most merciful, most benevolent;

I thank You.

I am indebted to many people for their support as I decided to further study. Firstly, I would like to thank my wife, for her constant and limitless support over the last few years. Her words of encouragement and advice have been the major push factors for my success; I could not have done this without her. I am also extremely grateful of my parents and siblings for the understanding and tolerance. I am especially thankful to my mentors who also my advisors, Dr Muhamad Noor Harun and Dr Ardiyansyah Syahrom for their guidance in all aspects of the work contained in this thesis. Advices, comments and critics of my work have made me stronger and a more accomplished researcher. I could not have composed this thesis without their tireless efforts. Not to forget, my special thanks go to Prof. Mohamed Rafiq Abdul Kadir for his many contributions. I would also like to thank all members of Medical Devices and Technology Group (MEDITEG) and Sports Innovation and Technology Centre (SITC) for their assistance over the last few years. It has been a pleasure to work with all of you and the experience has undoubtedly made me a better person. Finally, I'd like to thank all of people who have been direct or indirectly allow for this study to be accomplished, contributing ideas and expertise, and providing excellent services, amenities and an enjoying environment throughout my study.

“Anyone who has never made a mistake never tried anything new.”

- Albert Einstein

ABSTRACT

Biomechanics of bone has drawn major concern in research due to social and economic demand. In real life, trabecular bone is subjected to multiaxial stresses during routine physiological loading. Fatigue failure of the bone accounts for various clinical implications, thus studies and research to better understand the fatigue failure of the bone are needed. The overall aim of this study is to investigate the effect of torsional loading towards trabecular behaviour under compression in both monotonic and fatigue loading. Samples from femoral bovine trabecular bone were subjected to a series of monotonic and cyclic tests. Hill's criterion was selected to determine the five combined stress ratio of compressive to shear stress for fatigue test. For finite element simulation, effect of morphology and orientation were investigated to predict fatigue life and plastic strain. The ultimate stress of the trabecular bone in monotonic compression and torsion were 14.22 and 8.95 MPa, respectively. In monotonic multiaxial loading, the ultimate stress was reduced to 2.5 MPa in compression and 3.8 MPa in torsion. Under fatigue compression, an endurance limit was found approximately at 25 % of ultimate compressive stress. Under multiaxial fatigue, the ability of the sample to retain shear stiffness with increased number of cycles is strongly correlated to the stress ratio. Fatigue life reduction was significant when the maximum shear stress is at least 24 % of the maximum compression stress. From the computational analysis, it was demonstrated that lower bone volume fraction (BV/TV), trabecular thickness (Tb.Th), and connectivity density (Conn.D) resulted in lower number of cycles to failure, regardless to the loading conditions. However, the number of cycles to failure was found to be negatively correlated to the value of structural model index (SMI). Off-axis orientation effect on the fatigue life of the trabecular bone was demonstrated the worst in horizontal trabecular bone model. In conclusion, the effect of torsional loading onto the mechanical behaviour of bovine trabecular bone was demonstrated throughout this study. It is apparent that torsional forces are the major factor that needs to be considered since these can lead to fatigue fractures. This research is expected to improve the knowledge base for the development of trabecular bone analogous materials.

ABSTRAK

Penyelidikan biomekanik tulang telah mendapat perhatian luas disebabkan oleh tuntutan sosial dan ekonomi. Secara keseluruhannya, pengajian ini bertujuan untuk menyiasat kesan beban kilasan terhadap kelakuan tulang trabekular di bawah mampatan beban monotonik dan kelesuan. Sampel daripada tulang trabekular dari paha sapi telah dikenakan satu siri ujikaji monotonik dan kitaran. Kriteria Hill telah dipilih untuk menentukan lima nisbah kombinasi tekanan untuk ujian kelesuan. Untuk simulasi unsur terhingga, kesan morfologi dan orientasi telah disiasat untuk meramalkan hayat lesu dan keterikan plastik. Tekanan maksimum tulang trabekular dalam mampatan dan kilasan monotonik adalah masing-masing 14.22 dan 8.95 MPa. Dalam tekanan monotonik pelbagai paksi, tekanan maksimum telah berkurang kepada 2.5 MPa untuk mampatan dan 3.8 MPa untuk kilasan. Di bawah mampatan lesu, had kelesuan adalah lebih kurang 25 peratus dari tekanan mampatan maksimum. Di bawah kelesuan pelbagai paksi, kebolehpayaan sampel untuk menanggung kerichan dengan peningkatan bilangan kitaran adalah sangat dipengaruhi oleh nisbah tekanan. Penurunan hayat lesu adalah jelas apabila daya ricih maksimum pada sekurang-kurangnya 24 peratus dari tekanan mampatan maksimum. Dari analisis komputer telah menunjukkan bahawa nilai pecahan isipadu tulang (BV/TV), tebal trabekular (Tb.Th), dan ketumpatan sambungan (Conn.D) yang rendah mengakibatkan bilangan kitaran kegagalan yang rendah. Walau bagaimanapun, bilangan kitaran kegagalan adalah berkadar negative dengan nilai index struktur model (SMI). Kesan orientasi di luar paksi terhadap hayat lesu tulang trabekular telah ditunjukkan paling teruk dalam model tulang trabekular arah melintang. Kesimpulannya, kesan bebanan kilasan terhadap kelakuan mekanikal tulang trabekular sapi telah ditunjukkan dalam pengajian ini. Ianya jelas bahawa daya kilasan merupakan faktor utama yang harus diberi perhatian kerana menyumbang kepada fraktur kelesuan.

TABLE OF CONTENTS

CHAPTER	TITLE	PAGE
	DECLARATION	ii
	DEDICATION	iii
	ACKNOWLEDGEMENT	iv
	ABSTRACT	v
	ABSTRAK	vi
	TABLE OF CONTENTS	vii
	LIST OF TABLES	xi
	LIST OF FIGURES	xiii
	LIST OF ABBREVIATIONS	xix
	LIST OF SYMBOLS	xxi
	LIST OF APPENDICES	xxiii
1	INTRODUCTION	1
	1.1 Background of the Study	1
	1.2 Problem Statement	3
	1.3 Objectives	5
	1.4 Scope of Study	6
	1.5 Significances and Original Contributions of This Study	7
	1.6 Thesis Structure and Organization	8
2	LITERATURE REVIEW	10

2.1	Introduction	10
2.2	Bone: The Skeletal System	11
2.3	Bone Mechanics	22
2.3.1	Mechanical Properties	22
2.3.2	Fatigue Properties	28
2.3.3	Multiaxial Behaviour of Trabecular Bone	36
2.4	FE Analysis of Trabecular Bone	41
2.5	Summary	44
3	METHODOLOGY	46
3.1	Introduction	46
3.2	Sample Preparation	47
3.3	Mechanical Testing	51
3.3.1	Experimental Setup	51
3.3.2	Monotonic test	52
3.3.3	Fatigue test	53
3.4	Computational Analysis	55
3.4.1	Morphological Measurement	56
3.4.2	Reconstruction of 3D Model	59
3.4.3	Finite Element (FE) Analysis	61
3.4.4	Validation of FE simulation	66
3.5	Microstructural Characterization	70
3.6	Data analysis	71
3.6.1	Monotonic testing	71
3.6.2	Fatigue testing	76
3.6.3	Statistical Analysis	79
3.7	Summary	79

4	MECHANICAL BEHAVIOUR OF BOVINE TRABECULAR BONE	80
	4.1 Introduction	80
	4.2 Results and Discussion	81
	4.2.1 Compressive Behaviour of Bovine Trabecular Bone	81
	4.2.2 Effects of Superpositioned Torsional Load onto the Behaviour of Bovine Trabecular Bone under Monotonic Compression	85
	4.2.3 Failure Surface of Bovine Trabecular Bone	88
	4.3 Summary	92
5	FATIGUE BEHAVIOUR OF BOVINE TRABECULAR BONE	93
	5.1 Introduction	93
	5.2 Results and Discussion	94
	5.2.1 Fatigue Compressive Behaviour of Bovine Trabecular Bone.	94
	5.2.2 Fatigue Behaviour of Bovine Trabecular Bone under Combined Compression-Torsion	100
	5.3 Summary	113
6	COMPUTATIONAL ANALYSIS ON FATIGUE BEHAVIOUR OF BOVINE TRABECULAR BONE	114
	6.1 Introduction	114
	6.2 Results and Discussion	115
	6.3 Summary	122
7	CONCLUSION AND FUTURE RECOMMENDATION	123
	7.1 Conclusion	123

7.2 Limitation and Future Recommendation	126
REFERENCES	127
Appendices A-G	149 - 179

LIST OF TABLES

TABLE NO.	TITLE	PAGE
2.1	Definition of morphological parameters for trabecular bone sample which can be obtained from Bone J analysis in Image J.	16
2.2	Variation in trabecular parameters studies on human bone.	17
2.3	Various morphological parameters on various animals.	18
2.4	Young's modulus definition and strain measurement in the literature.	19
2.5	Different strain rates used in reported literature for estimation of trabecular bone properties.	21
2.6	Comparison of several fatigue parameters from previous researchers.	24
3.1	Ultimate stress values for each loading state.	55
3.2	List of Bone J commands for the trabeculae [56]. The latest available commands can be found on http://bonej.org/ .	57
3.3	Parameters used in fatigue modelling of trabecular bone.	65
3.4	Microstructural parameter of the samples	66
4.1	<i>p</i> -value, mean, S.D. and range of values for compressive properties of the bovine trabecular bone.	83

4.2	Compressive-torsional properties of bovine trabecular bone.	86
4.3	<i>p</i> -value, mean, S.D. and range of values for torsional properties of the bovine trabecular bone.	90
5.1	Comparison of fatigue experimental lifetime curve across sites and species by various loading modes.	99
5.2	Summary of the lifetime curve obtained in different stress states.	107
6.1	Microstructural parameters of trabecular bone samples with coefficient of determination (R^2) and <i>p</i> -value in relation to cycles to failure, N_f in both uniaxial and multiaxial loading conditions.	117
6.2	Coefficient of determination for microstructural parameters of trabecular bone samples and <i>p</i> -value relative to effective plastic strain in both uniaxial and multiaxial loading condition.	117
7.1	The list of limitations of this study and the corresponding recommendations for future work.	126

LIST OF FIGURES

FIGURE NO.	TITLE	PAGE
1.1	Fracture and treatment of an injured femur. (a) Spiral fracture of long femoral bone and separated femoral head, (b) treatment of the femoral fracture after operation, and (c) stress distribution of femoral implant and screws.	5
1.2	Thesis organisation roadmap.	9
2.1	Classification of human bone according to type and shape.	11
2.2	Bone structure at different length scale in hierarchical order.	12
2.3	Bone remodelling cycle. Adapted from [49].	13
2.4	Typical scanning electron micrograph (SEM) image of trabecular bone surface showing structure with many complexly arranged trabecular struts.	14
2.5	Femoral bone with entrapped marrow (red box) and without marrow (black box) at different trabecular region.	15
2.6	Typical stress-strain curve of trabecular bone showing elastic-plastic region with offset line.	23
2.7	Sequence of cyclic deformation and fatigue damage [95].	30
2.8	Example of stress and number of cycles (S-N) curve for aluminium and carbon steel.	31

2.9	Example of strain-life curve.	32
2.10	Typical failure envelope of yield behaviour in plane strain determined from a high-resolution finite element models. Adapted from [180].	37
3.1	Research framework.	47
3.2	Excision lines on the femur oriented to the bone axis. This figure is a representation only.	49
3.3	Cored samples from sectioned bone with the top and side views of cleaned sample.	50
3.4	Schematic representation of the experimental setup. Mounted sample ends were fixed and glued into stainless steel caps and secured with a pin screw to minimize end effects.	52
3.5	Typical fatigue waveform applied for simultaneous compression-torsion.	54
3.6	Skyscan 1172 micro-computed tomography scans equipment.	56
3.7	Data obtained from micro-CT with (a) shows raw scanned image files and (b) demonstrates the image files are stacked in sequence accordingly to the scanned sample orientation.	58
3.8	Morphological measurements for Tb.Sp and Tb.Th by Image J.	58
3.9	2D micro-CT images dataset for trabecular bone and whole reconstructed trabecular structure.	59
3.10	Trabecular 3D model construction using (a) AMIRA software, and (b) mesh surface editing in MIMICS.	60
3.11	Mesh surface of trabecular model (a) before and (b) after post-editing for FE simulation.	60
3.12	Reconstructed 3D trabecular bone model being excised to sub-volume ROI which high in resolution but small in size.	61
3.13	Typical of boundary condition setting in the finite element analysis.	63

3.14	Three different models extracted from whole sample with different orientations: vertical (yellow), horizontal (white) and 45 degree (black).	64
3.15	Typical example of cyclic plasticity model with different tangent modulus (red: $0.01E_0$ and black: $0.05E_0$) in low and high load level of fully reversed loading cycle to validate the elastoplasticity model with model from Garcia et al. [223].	67
3.16	Evolution of plastic strain with time at the point evaluation with controlled fine mesh.	67
3.17	Convergence formulation with regard to the normalized modulus (E/E_0).	68
3.18	Comparison between FE simulation and experimental modulus with periodic boundary condition.	69
3.19	The S-N relationship of vertical models subjected to normal stress amplitude.	70
3.20	FESEM equipment used for sample surface and fracture characterization.	71
3.21	Typical stress-strain curve with representation of mechanical properties; the Young's modulus, E , the yield stress, σ_{yc} , the ultimate stress, σ_{ultc} , and the yield strain, ε_{yc} .	72
3.22	Relationships of (a) torque with rotational deformation, and (b) shear stress with shear strain generated by torsion test.	74
3.23	Typical relationship of stress-strain hysteresis for pure compressive fatigue with determination of secant modulus, total strain and residual strain.	77
4.1	Typical compressive stress-strain relationship of bovine trabecular bone with 0.2 % offset yield criteria.	82
4.2	Correlation in between the sample density and compressive properties, of which (a) Young's	

	modulus; (b) initial yield stress; (c) ultimate stress; and (d) yield strain.	84
4.3	The relationship of compressive modulus and yield strength of bovine trabecular bone.	84
4.4	Effect of superpositioned torsional loading on compressive stress-strain relationship of bovine trabecular bone.	86
4.5	Comparison of modulus-density relationship in between samples underwent uniaxial compression and those of combined loading.	87
4.6	Correlation in between the compressive yield strength at 0.2 % offset and the modulus of samples under combined loading.	88
4.7	Torsional characteristic of bovine trabecular bone with; (a) typical torque–rotational deformation curve, and (b) representation of the shear stress and shear strain curve with the offset yield criteria.	89
4.8	Correlation in between sample density and shear properties of which; (a) shear modulus; (b) maximum shear stress; and (c) shear yield strain, while in (d) shows correlation between shear modulus and shear stress in torsion.	90
4.9	Failure surface of the samples under combined monotonic compression-torsion fitted to various failure criteria of trabecular samples on stress space.	91
5.1	The stress-strain hysteresis loops of bovine trabecular bone sample subjected to fatigue compression. ($\sigma/E_o =$ 0.0478 , $N_f = 173,333$), The residual strain is the plastic deformation over increasing strain, while maximum strains are equivalent to the total strains (residual strain and strains in elastic region, combined).	95
5.2	Damage evolution ($1-D$) of bovine trabecular bone sample.	96

5.3	Strain accumulation with throughout the number of cycles ($\sigma/E_o = 0.0052$). Deformation stages are marked by I, II and III.	97
5.4	Relationship of normalized stress and number of cycles to failure of bovine trabecular bone sample under fatigue compression.	98
5.5	SEM micrographs of (a) the fracture surface on a trabecular sample after about one million cycles in compression, and (b) a trabecular strut from the same sample at higher magnification with evident microcracking.	100
5.6	Schematic representation of Hill's criterion curve and stress ratio determination concept. The point 'P' is the stress ratio expressed in terms of (x, y) coordinates at angle θ , in which a particular stress state lies.	101
5.7	The stress-strain diagrams from combined compression-torsion test for CT at 25 % N_f (a) for compression, and (b) for torsion.	102
5.8	Shear modulus reduction profile of bovine trabecular bone at various stress levels for (a) T, (b) TD, (c) CT, and (d) CD.	104
5.9	Compressive modulus profile of bovine trabecular bone at all stresses levels for CD.	105
5.10	The number of cycles to failure at all stresses states.	106
5.11	Monotonic compressive and combined fatigue compressive-shear strength.	109
5.12	FESEM micrograph of a sample under compression-torsion with loading combination of CD at 50 %, with observations on (a) surface fracture, (b) microcracks on struts, (c) microfracture on individual strut, and (d) buckling effect.	110
5.13	SEM micrograph of trabecular sample subjected to combined compression-torsion loading. (a) Fracture line of the sample (at 100 μ m), (b) fracture surface of	

	the sample (at 1mm), (c) icicle-like fracture of a trabeculae with stump structure left (at 10 μ m), and (d) delaminating effect on sample surface (at 100 μ m).	
	Failure occurred is mostly shear-dominated.	111
5.14	Series of SEM images of collapsed struts.	112
6.1	Linear relationship between (a) BV/TV and (b) SMI with cycles to failure, N_f .	116
6.2	Comparison of (a) uniaxial and (b) multiaxial life prediction of the models at different trabecular orientation.	118
6.3	Difference in von-Mises stress distribution of trabecular surface corresponding to trabecular orientations; (a) vertical (b) horizontal, and (c) 45° subjected to uniaxial loading.	119
6.4	Difference in von-Mises stress distribution of the trabecular bone surface corresponding to trabecular bone orientations; (a) vertical (b) horizontal, and (c) 45° subjected to multiaxial loading.	120
6.5	Effective plastic strain values for the corresponding trabecular models at different orientation.	121

LIST OF ABBREVIATIONS

ASTM International	-	American Society for Testing and Materials
Micro-CT	-	Micro-computed tomography
BV/TV	-	Bone volume fraction
Tb.Th	-	Trabecular thickness
Tb.Sp	-	Trabecular space
Tb.N	-	Trabecular number
FE	-	Finite element
HA	-	Hydroxyapatite
BMD	-	Bone mineral density
3D	-	Three-dimensional
ZIB	-	Zuse Institute Berlin
US	-	United States
NA	-	Not applicable
S-N	-	Stress-life
FEM	-	Finite element method
LCF	-	Low-cycle fatigue
HCF	-	High-cycle fatigue
2D	-	Two-dimensional
SMI	-	Structural model index
Conn.D	-	Connectivity density
DA	-	Degree of anisotropy
P	-	Plate-like trabeculae
R	-	Rod-like trabeculae
ROI	-	Region of interest

FESEM	-	Field emission scanning electron microscopy
SEM	-	Scanning electron microscopy
SD	-	Standard deviation

LIST OF SYMBOLS

$\Delta\sigma$	-	Stress range
N_f	-	Number of cycles to failure
N	-	Number of cycles
σ_f	-	Fatigue strength coefficient
b	-	Basquin's exponent
$\Delta\varepsilon$	-	Strain range
ε_f	-	Fatigue ductility coefficient
c	-	Fatigue ductility exponent
N_t	-	Transition of life
σ	-	Stress
ε	-	Strain
E	-	Modulus
R^2	-	Regression coefficient
n	-	Number of sample
σ_i	-	Principal stress direction
σ_{eq}	-	Equivalent von Mises stress
Y_A	-	Uniaxial yield strength
Y_S	-	Shear yield strength
p	-	Significance level of the test
σ_{yc}	-	Compressive yield strength
σ_{ultc}	-	Ultimate or maximum compressive strength
σ_{max}	-	Maximum stress
σ_{min}	-	Minimum stress
ε_{max}	-	Maximum strain
ε_{min}	-	Minimum strain

τ	-	Shear stress
γ	-	Shear strain
k	-	Torsional modulus
G	-	Shear modulus or modulus of rigidity
T	-	Torque / torsion
τ_{\max}	-	Maximum shear stress
C	-	Compression/ compressive
E_{kin}	-	Kinematic hardening modulus

LIST OF APPENDICES

APPENDIX	TITLE	PAGE
A	Sample of trend data analysis in static	150
B	Sample of trend data analysis in fatigue	156
C	Sample of tracking data analysis in fatigue loading	161
D	Sample of data analysis in compression-torsion fatigue	167
E	Sample of normalized modulus with number of cycles	169
F	Sample of modulus loss in compression and torsion	172
G	List of publications	177

CHAPTER 1

INTRODUCTION

1.1 Background of the Study

For over 30 years biomechanics research has been widely explored with special interest is sending forth on the influence of trabecular bone towards weakening and failure of whole bone, and how the stimulating remodelling process helps in retaining the bone strength [1]. Clear understanding of the biomechanics of bone is well related in diagnosis and treatment of medical issues such as osteoporosis, bone fracture, bone remodelling, and implant system. Biomechanics of bone has drawn major concern in research due to social and economic demand [2]. Proper understanding of bone mechanics is required to tackle various medical issues. The mechanical behaviour of bone related to its architecture will improve clinical practise in diagnosing osteoporosis. Further evaluation on damage evolution in bone will provide information on dimmed principles of mechanobiology. From here, development of implants can be enhanced while prostheses design and systems will be able to function usefully. On top of that, treatment necessary for defects or complex fractures which usually involve patients at old ages can be developed. At instant, there are interesting alternatives have been proposed in order to tackle issues with bone defects [3, 4], however without prior profound knowledge on the bone itself, these approaches remain speculative.

Failure in most loaded engineering structures has been characterized as fatigue-induced [5]. Fatigue can be defined as the weakening of a material resulted from repetitive applied stresses or strains. Stephens et al. (2000) [6] highlighted six key words from ASTM International (American Society for Testing and Materials) definition of fatigue which imply the process of fatigue in a material, i.e. progressive, localized, permanent, fluctuating, cracks, and fractures. In general, this process involves the nucleation and growth of cracks to final fracture. Fatigue failure in bone has been found to be resulted from worsened deposition or mineralisation of bone matrix, or the unrepaired microdamage accumulation from daily repetitive loads which increase bone fragility [7, 8]. Such failure, while most presented in elderly patients, is also associated with stress fractures [9] in younger people with increase load beyond the bone capacity to remodel. Fatigue failure in bone starts with microcracks initiation, in which occur in regions of high strain and accumulate with increased number of cycles or increased strain. These cracks are often repaired during the remodelling process. However, failed microcracks grow and propagate as a result of interlamellar stresses generated at its tip. As the bone stiffness declines, damage is accumulated rapidly and ultimate failure of the structure occurs as fatigue progresses faster than the rate of remodelling. Despite the known capability of remodelling process to limit bone fragility and to prevent failure caused by microdamage, under-capacity of this process – or lagging response towards elevated load puts the associated bone at risk of sudden fracture. Furthermore, remodelling induction capacity is diminished with age [10].

As fatigue failure in bones contribute to significant clinical implications, studies and investigations to better comprehend fatigue failure in bones are required. Factors affecting fatigue strength of bone include the loading mechanism, frequency, strain rate, age, anatomic site, stiffness, density and temperature, as well as the microstructure of the bone [11]. With advancement of technology, direct quantitative morphological analysis on three-dimensional (3D) reconstructions is made possible with micro-computed tomography (micro-CT). The morphological indices included volume fraction (BV/TV), trabecular thickness (Tb.Th), trabecular separation (Tb.Sp), and trabecular number (Tb.N). As material testing on highly inhomogeneous structures like the trabecular bone is quite complicated and no

standard for the experimental conditions are given in terms of sample size, loading rate, loading mode, and surrounding media, results from literature are also diversified. Some of the variations in mechanical data may be ascribed to experimental effects, introduced by ignoring the structural anisotropy, the proper boundary conditions (e.g. end artefact errors) [12, 13] and size effects [14]. But there is also a natural heterogeneity which complicates the analysis of trabecular bone and large variation in between samples properties may scattered the results in mechanical interpretation especially in bone mechanic study such as creep or fatigue [15].

Progressive collapses of the vertebrae [16] and loosening of implants [17] have been associated to the damage and creep strain which attracts interest in understanding the associated failure. The number of cycles to failure of the trabecular is in direct relationship with the volume fraction, fabric, and applied stress [18]. Lifetime of the trabecular has also been recognised to be influenced by loading direction [19]. Current fatigue assessment on trabecular bone is limited to uniaxial compression. While physiological and traumatic loading are multiaxial in nature, uniaxial assessment limits the reliability of the yielded information. To the author's knowledge, none of the reported works in the literature has ever quantified the behaviour of the trabecular under multiaxial fatigue. Therefore, the outcomes of this present work is hope to shed lights on a few aspects involved in the failure of the trabecular under combined fatigue compression-torsion and contribute information for future development.

1.2 Problem Statement

Bone fracture [20, 21], age-related fragility fractures [8], and implants loosening [17] have been found to be originated by fatigue damage. However, fatigue behaviour of trabecular bone has received only few attentions [18, 22-27]. Even so, these studies are conducted under uniaxial compressive loading, in which may badly align with in vivo physiological off-axis loading directions [28, 29]. This

off-axis loading is influenced by trabecular microarchitectural properties, which are also attributed to osteoporosis. Osteoporosis promote bone fragility and increase the bone's susceptibility to fracture, which has been reported to strike at trabecular bone dominant sites such as hip, spine, and wrist. As the lifespan increases, assessment on bone failure risk becomes more significant. Current practice in osteoporosis assessment determines failure risk of bone by measuring the bone mineral density (BMD). This method however leaves out other contributing factors to the strength of bone such as the morphological information. Furthermore, the feverish lifestyle of older people nowadays has also increase the need of implants and prostheses. Implant loosening has been associated as one of the factor of failure in total hip replacement surgery [30-32] which is associated to the reduction of mechanical competency of the immediate adjacent trabecular [33-35]. As the cost of second surgical procedure is reported to be three times as expensive as the preliminary ones [36], factors such as changes in the trabecular quality with age and osseous-integration process must be well assessed to get the replacement done right the first time [30, 37]. Furthermore, implant systems may also alter the local loading conditions (Figure 1.1). However, research efforts in this area require participation of joined expertise, given the complexity of the problems. Thus, understanding the fatigue properties of bone may provide information on osteoporotic bone behaviour toward normal physiological loading and its associated diagnosis and treatment, as well as improve implant systems in terms of material selection, placement, and etc.

Bone is subjected to multiaxial stresses and strains *in vivo* [9, 38-40] while less to none known multiaxial fatigue evaluation on trabecular bone has ever be done. Uniaxial loading alone is insufficient to provide the necessary information in bone failure prediction as different failure mode is observed to that of under multiaxial loading. Multiaxial loading demonstrates mixed-mode failure where the damage propagated from one mode (tension) to another (shear). In bioengineering, multiaxial criterion provide better understanding on the relationship of the trabecular tissue structure and its physiology in which will improved implant system and development of bone analogue [41]. Therefore, current work may comprise the following research questions;

- Why previously reported mechanical evaluation failed to describe well of the trabecular bone failure?
- What is the influence of torsional loading on the behaviour of trabecular bone under compressive fatigue and monotonic loading?
- How do the morphology, anatomical site, and orientation affect the trabecular behaviour under multiaxial fatigue loading?

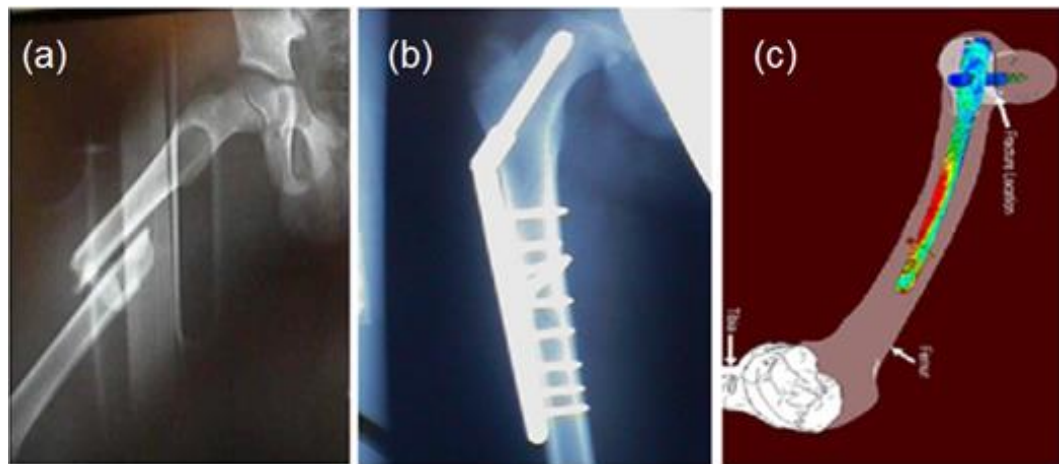


Figure 1.1 Fracture and treatment of an injured femur. (a) Spiral fracture of long femoral bone and separated femoral head, (b) treatment of the femoral fracture after operation, and (c) stress distribution of femoral implant and screws.

1.3 Objectives

Human bone deformed in terms of its microstructural and ultrastructural features with age [8, 42, 43]. In vivo, physiological loading subjected to the bone change microstructural response and thus alter the failure behaviour, stress or strain magnitude as well as loading mode. As the assessments on bone failure under physiological condition with relevant multiaxial loading are scarcely done, damage mechanism of bone, particularly the trabecular structure, remain poorly understood. Furthermore, a strong experimental base is in need to accommodate current advanced numerical models application [44, 45] and theoretical model for deformation

processes. Thus, the overall aim of this study is to investigate the effect of torsional loading towards trabecular behaviour under compression in both monotonic and fatigue loading. The specific objectives of the study are;

1. to investigate the effect of superimposed torsional loading onto the monotonic compressive properties of bovine trabecular bone,
2. to evaluate the torsional loading effects onto the fatigue compressive behaviour of bovine trabecular bone, and
3. to simulate compressive fatigue life and investigate the effect of morphological parameters and sample orientation.

1.4 Scope of Study

Sample of trabecular bone in this study has been gathered and extracted from bovine proximal femur from mediolateral femoral condyles, neck of femur and greater trochanter. This study is divided into two important parts: experiment and computational simulation. The scope of the present study can be summarised as follows;

- i. Sample used was extracted from bovine (cow) bone which used in femoral head, neck, and medial-lateral condyles.
- ii. Micro-computed tomography (μ -CT) scanned of sample.
- iii. Monotonic test: Pure compression, pure torsion, and combined compression-torsion test.
- iv. Fatigue test: Pure compression, pure torsion, and combined compression-torsion test with five different stress ratios.
- v. Software used for morphology measurement: Image J.
- vi. Software used for 3D reconstruction: Mimics 10.01 and AMIRA 4.0.
- vii. Software used for finite element analysis: COMSOL Multiphysics 3.4.
- viii. Parameter study of the effect of morphology and orientation (vertical, 45 degree, and horizontal)

The study focuses on the effects of multiaxial and torsional loading imposed on trabecular bone structure that probably represent realistic condition adapted during normal physiological loading. Evaluation is associated more into compression fatigue behaviour of trabecular bone. However, details study on the fracture behaviour is not included. Torsional analysis in both monotonic and fatigue part were also excluded.

1.5 Significances and Original Contributions of This Study

Both cortical and trabecular bone have been investigated in terms of their mechanical properties and behaviour upon loading [11, 18, 23-25, 39, 43, 46]. Even though current study investigates trabecular bone exclusively, the mechanics of both types of bones share relevant properties that are complementary to each other. A close relationship in between age-related fragility fractures and stress fracture among youngsters is worth of notice. Microdamage in bone with normal routine can be repaired approximately at the same rate as the accumulation of damage, thus fractures can be avoided. However, with elevated loading as in athletes and army routine, bone microdamage accumulates at higher rate than normal remodelling capacity and often results in failure. As the fracture mechanics of stress fracture are very similar to that of osteoporosis, it is believed that much of the subject presented in current study can contribute to both medical issues and help in improving diagnostic and treatment aspects of the bone related diseases.

Fatigue progressive failure in trabecular bone has been associated with the loosening of implants [47] and other non-traumatic fractures. Complex loading conditions may be presented in vivo, thus multiaxial criteria for trabecular bone is of significant interest. Furthermore, traumatic injuries usually induce off-axis loading. Therefore, present work focused on quantification of the trabecular behaviour under multiaxial fatigue to improve validity and accuracy of the trabecular failure prediction, which was failed to be presented by previous uniaxial assessment. From

here, the effect of torsional loading onto the fatigue compression properties of the trabecular is presented. The study was extended to numerical analyses of microarchitectural parameters and loading orientation by finite element (FE).

1.6 Thesis Structure and Organization

This thesis is composed of seven chapters (Figure 1.2). Chapter 1 is an introduction, which consists of research background, scope of research, objectives of the study, research significance, problems statement, and organisation of the thesis. Chapter 2 is the literature review. The reviews included are from literatures of the recent twenty years, in which critically assessed to support the aforementioned research objectives. Chapter 3 presents the methodology in general from the procedure for sample preparation to data analyses. However, specific methodology for a particular experimental or computational evaluation is presented separately in its associated section. Elaborated assessment for monotonic response of the trabecular samples are delivered in Chapter 4. This chapter is divided into three sections; the monotonic assessment of trabecular samples under compression and torsion, the effects of superimposed torsional loading on monotonic compression evaluation, and the effects of combined monotonic compression-torsion on the samples properties. The main subject of research interest is presented in Chapter 5 which divided into several sections of fatigue assessment. The assessment starts with uniaxial fatigue evaluation, follows by the trabecular response towards superimposed torsion on fatigue compression. This chapter ends with combined compression-torsion fatigue evaluation. In Chapter 6, the computational simulation analyses are presented. The first section demonstrates the trabecular response towards loading mode based on the anatomical sites and morphological indices. Then, the study is extended to clarify the effects of samples orientation and fatigue life assessment which compares the prediction for uniaxial and that of multiaxial loading. At last, Chapter 7 describes general conclusion drew from the whole study, discusses limitations of this study and recommendation for improvement in future works.

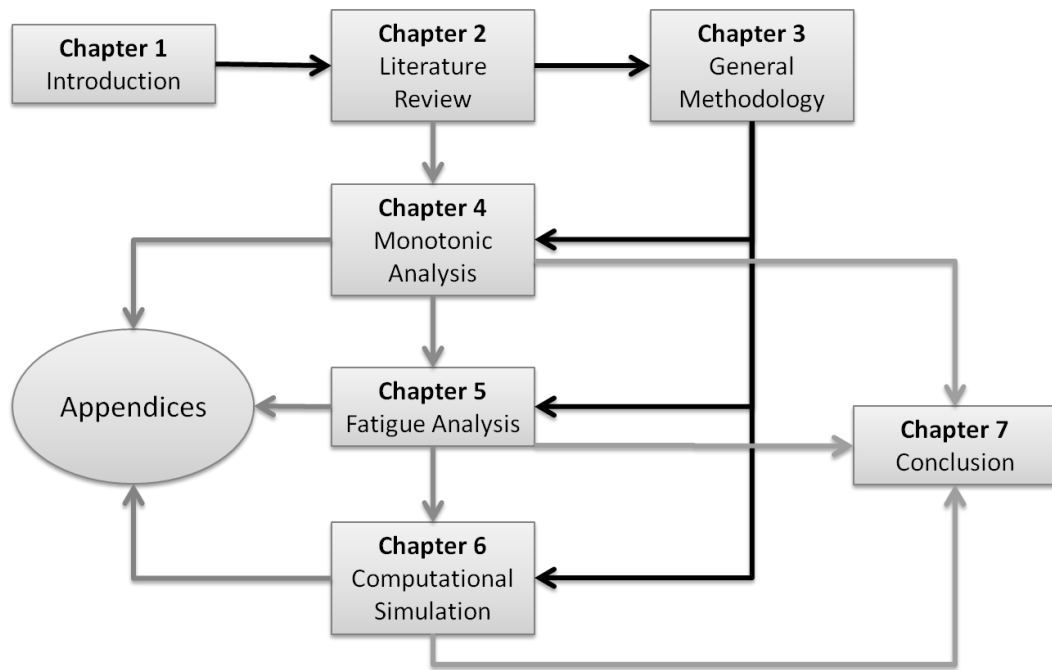


Figure 1.2 Thesis organisation roadmap.

REFERENCES

1. Keaveny, T.M., et al. Biomechanics of trabecular bone. *Annual Review of Biomedical Engineering*. 2001. **3**: p. 307-333.
2. Office of the Surgeon, G., *Reports of the Surgeon General*, in *Bone Health and Osteoporosis: A Report of the Surgeon General*. 2004, Office of the Surgeon General (US): Rockville (MD).
3. Li, J.P., et al. Cancellous bone from porous Ti6Al4V by multiple coating technique. *J Mater Sci Mater Med*. 2006. **17**(2): p. 179-85.
4. Englert, C., et al. Conductive bone substitute material with variable antibiotic delivery. *Unfallchirurg*. 2007. **110**(5): p. 408-13.
5. Suresh, S. *Fatigue of Materials*. 1998: Cambridge University Press.
6. Stephens, R.I., et al. *Metal Fatigue in Engineering*. 2000: John Wiley & Sons.
7. Burr, D.B., et al. Bone remodeling in response to in vivo fatigue microdamage. *J Biomech*. 1985. **18**(3): p. 189-200.
8. Burr, D.B., et al. Bone Microdamage and Skeletal Fragility in Osteoporotic and Stress Fractures. *J Bone Miner Res*. 1997. **12**(1): p. 6-15.
9. Burr, D.B., et al. In vivo measurement of human tibial strains during vigorous activity. *Bone*. 1996. **18**(5): p. 405-410.
10. Waldorff, E.I., S.A. Goldstein, and B.R. McCreadie. Age-dependent microdamage removal following mechanically induced microdamage in trabecular bone in vivo. *Bone*. **40**(2): p. 425-432.
11. Choi, K. and S.A. Goldstein. A comparison of the fatigue behavior of human trabecular and cortical bone tissue. *J Biomech*. 1992. **25**(12): p. 1371-1381.
12. Linde, F. and I. Hvid. Stiffness behaviour of trabecular bone specimens. *J Biomech*. 1987. **20**(1): p. 83-89.

13. Keaveny, T.M., et al. Systematic and random errors in compression testing of trabecular bone. *J Orthop Res.* 1997. **15**(1): p. 101-110.
14. Taylor, D. Scaling effects in the fatigue strength of bones from different animals. *J Theo Biol.* 2000. **206**(2): p. 299-306.
15. Makiyama, A.M., S. Vajjhala, and L.J. Gibson. Analysis of crack growth in a 3D voronoi structure: A model for fatigue in low density trabecular bone. *J Biomech Eng.* 2002. **124**(5): p. 512-20.
16. Goff, M., et al. Fatigue-induced microdamage in cancellous bone occurs distant from resorption cavities and trabecular surfaces. *Bone.* 2015.
17. Bauer, T.W. and J. Schils. The pathology of total joint arthroplasty.II. Mechanisms of implant failure. *Skeletal Radiol.* 1999. **28**(9): p. 483-97.
18. Rapillard, L., M. Charlebois, and P.K. Zysset. Compressive fatigue behavior of human vertebral trabecular bone. *J Biomech* 2006. **39**(11): p. 2133-2139.
19. Dendorfer, S., et al. Anisotropy of the fatigue behaviour of cancellous bone. *J Biomech.* 2008. **41**(3): p. 636-641.
20. Snyder, R.A., M.C. Koester, and W.R. Dunn. Epidemiology of stress fractures. *Clin Sports Med.* 2006. **25**(1): p. 37-52, viii.
21. Niemeyer, P., et al. Stress fractures in the juvenile skeletal system. *Int J Sports Med.* 2006. **27**(3): p. 242-9.
22. Yamamoto, E., et al. Development of residual strains in human vertebral trabecular bone after prolonged static and cyclic loading at low load levels. *J Biomech.* 2006. **39**(10): p. 1812-1818.
23. Michel, M.C., et al. Compressive fatigue behavior of bovine trabecular bone. *J Biomech* 1993. **26**(4-5): p. 453-463.
24. Moore, T.L. and L.J. Gibson. Fatigue of bovine trabecular bone. *J Biomech Eng.* 2003. **125**(6): p. 761-8.
25. Haddock, S.M., et al. Similarity in the fatigue behavior of trabecular bone across site and species. *J Biomech* 2004. **37**(2): p. 181-187.
26. Dendorfer, S., H.J. Maier, and J. Hammer. Fatigue damage in cancellous bone: An experimental approach from continuum to micro scale. *J Mech Behav Biomed Mater.* 2009. **2**(1): p. 113-119.

27. Lambers, F.M., et al. Microdamage caused by fatigue loading in human cancellous bone: Relationship to reductions in bone biomechanical performance. *PLoS One*. 2013. **8**(12): p. e83662.
28. Bergmann, G., et al. Hip contact forces and gait patterns from routine activities. *J Biomech* 2001. **34**(7): p. 859-871.
29. Homminga, J., et al. Cancellous bone mechanical properties from normals and patients with hip fractures differ on the structure level, not on the bone hard tissue level. *Bone*. 2002. **30**(5): p. 759-764.
30. Frost, H. Perspectives on artificial joint design. *Journal of long-term effects of medical implants*. 1991. **2**(1): p. 9-35.
31. Berry, D.J., et al. Twenty-five-year survivorship of two thousand consecutive primary Charnley total hip replacements. *J Bone Joint Surg*. 2002. **84**(2): p. 171-177.
32. Maher, S., P. Prendergast, and C. Lyons. Measurement of the migration of a cemented hip prosthesis in an in vitro test. *Clin Biomech*. 2001. **16**(4): p. 307-314.
33. Frost, H.M. A 2003 update of bone physiology and Wolff's law for clinicians. *The Angle orthodontist*. 2004. **74**(1): p. 3-15.
34. Taylor, M., et al. Cancellous bone stresses surrounding the femoral component of a hip prosthesis: an elastic-plastic finite element analysis. *Med Eng Phy*. 1995. **17**(7): p. 544-550.
35. Taylor, M. and K. Tanner. Fatigue failure of cancellous bone: a possible cause of implant migration and loosening. *J Bone Joint Surg*. 1997. **79**(2): p. 181-182.
36. Office, G.B.N.A., G.B.P.H.o. Commons, and N. Executive. *Hip Replacements: Getting It Right First Time*. 2000: Stationery Office.
37. Frost, H.M. Does bone design intend to minimize fatigue failures? A case for the affirmative. *J Bone Miner Metab*. 2000. **18**(5): p. 278-282.
38. Carter, D.R. Anisotropic analysis of strain rosette information from cortical bone. *J Biomech*. 1978. **11**(4): p. 199-202.
39. Vashishth, D., K. Tanner, and W. Bonfield. Fatigue of cortical bone under combined axial-torsional loading. *J Orthop Res*. 2001. **19**(3): p. 414-420.

40. Lotz, J., E. Cheal, and W. Hayes. Fracture prediction for the proximal femur using finite element models: part I—linear analysis. *J Biomech Eng.* 1991. **113**(4): p. 353-360.
41. Bayraktar, H.H., et al. The modified super-ellipsoid yield criterion for human trabecular bone. *J Biomech Eng.* 2004. **126**(6): p. 677-684.
42. Nyssen-Behets, C., P.-Y. Duchesne, and A. Dhem. Structural changes with aging in cortical bone of the human tibia. *Gerontology.* 1997. **43**(6): p. 316-325.
43. Zioupos, P. and J. Currey. Changes in the stiffness, strength, and toughness of human cortical bone with age. *Bone.* 1998. **22**(1): p. 57-66.
44. Yeni, Y.N., et al. Trabecular shear stress in human vertebral cancellous bone: Intra- and inter-individual variations. *J Biomech.* 2001. **34**(10): p. 1341-6.
45. Homminga, J., et al. The osteoporotic vertebral structure is well adapted to the loads of daily life, but not to infrequent “error” loads. *Bone.* 2004. **34**(3): p. 510-516.
46. Allard, R.N., *Mechanical compression testing to determine the elastic modulus of cancellous bone.* 1990, The University of Texas at Arlington: United States -- Texas.
47. Bauer, T.W. and J. Schils. The pathology of total joint arthroplasty. *Skeletal Radiol.* 1999. **28**(9): p. 483-497.
48. Starr, C. *Biology: Concepts and Applications.* 2002: Cengage Learning.
49. Oftadeh, R., et al. Biomechanics and mechanobiology of trabecular bone: A review. *J Biomech Eng.* 2015. **137**(1).
50. Samuel, S.P., C.S.U.D.o. Chemical, and B. Engineering. *Fluid/solid interactions in cancellous bone.* 2005: Cleveland State University.
51. Turunen, M.J., et al. Composition and microarchitecture of human trabecular bone change with age and differ between anatomical locations. *Bone.* 2013. **54**(1): p. 118-125.
52. Banse, X., et al. Inhomogeneity of human vertebral cancellous bone: Systematic density and structure patterns inside the vertebral body. *Bone.* 2001. **28**(5): p. 563-571.

53. Hulme, P., S. Boyd, and S. Ferguson. Regional variation in vertebral bone morphology and its contribution to vertebral fracture strength. *Bone*. 2007. **41**(6): p. 946-957.
54. Lin, J.C., et al. Heterogeneity of trabecular bone structure in the calcaneus using magnetic resonance imaging. *Osteoporosis Int*. 1998. **8**(1): p. 16-24.
55. Bevill, G., F. Farhamand, and T.M. Keaveny. Heterogeneity of yield strain in low-density versus high-density human trabecular bone. *J Biomech*. 2009. **42**(13): p. 2165-2170.
56. Doube, M., et al. BoneJ: Free and extensible bone image analysis in ImageJ. *Bone*. 2010. **47**(6): p. 1076-1079.
57. Odgaard, A. Three-dimensional methods for quantification of cancellous bone architecture. *Bone*. 1997. **20**(4): p. 315-328.
58. Hildebrand, T.O.R. and P. Rüeggsegger. Quantification of Bone Microarchitecture with the Structure Model Index. *Comput Methods Biomech Biomed Eng*. 1997. **1**(1): p. 15-23.
59. Dougherty, R. and K.H. Kunzelmann. Computing local thickness of 3D structures with ImageJ. *Microsc Microanal*. 2007. **13**(Supplement S02): p. 1678-1679.
60. Teo, J.C.M., et al. Correlation of cancellous bone microarchitectural parameters from microCT to CT number and bone mechanical properties. *Mater Sci Eng C*. 2007. **27**(2): p. 333-339.
61. Rho, J.Y., M.C. Hobatho, and R.B. Ashman. Relations of mechanical properties to density and CT numbers in human bone. *Med Eng Phys*. 1995. **17**(5): p. 347-355.
62. Nicholson, P.H.F., et al. Do quantitative ultrasound measurements reflect structure independently of density in human vertebral cancellous bone? *Bone*. 1998. **23**(5): p. 425-431.
63. Portero-Muzy, N., et al. Euler(strut.cavity), a new histomorphometric parameter of connectivity reflects bone strength and speed of sound in trabecular bone from human os calcis. *Calcif Tissue Int*. 2007. **81**(2): p. 92-98.

64. Hudelmaier, M., et al. Gender differences in trabecular bone architecture of the distal radius assessed with magnetic resonance imaging and implications for mechanical competence. *Osteoporosis Int.* 2005. **16**(9): p. 1124-1133.
65. Majumdar, S., et al. High-resolution magnetic resonance imaging: Three-dimensional trabecular bone architecture and biomechanical properties. *Bone.* 1998. **22**(5): p. 445-454.
66. Anderson, I.A. and J.B. Carman. How do changes to plate thickness, length, and face-connectivity affect femoral cancellous bone's density and surface area? An investigation using regular cellular models. *J Biomech* 2000. **33**(3): p. 327-335.
67. Goulet, R.W., et al. The relationship between the structural and orthogonal compressive properties of trabecular bone. *J Biomech.* 1994. **27**(4): p. 375-389.
68. Morgan, E.F., et al. Contribution of inter-site variations in architecture to trabecular bone apparent yield strains. *J Biomech* 2004. **37**(9): p. 1413-1420.
69. Kleerekoper, M., et al. The role of three-dimensional trabecular microstructure in the pathogenesis of vertebral compression fractures. *Calcif Tissue Int.* 1985. **37**(6): p. 594-597.
70. Hildebrand, T. and P. Rüegsegger. A new method for the model-independent assessment of thickness in three-dimensional images. *J Microsc.* 1997. **185**(1): p. 67-75.
71. Yeni, Y.N., et al. Trabecular shear stress amplification and variability in human vertebral cancellous bone: Relationship with age, gender, spine level and trabecular architecture. *Bone.* 2008. **42**(3): p. 591-596.
72. Nicholson, P.H.F. and R. Strelitzki. On the prediction of young's modulus in calcaneal cancellous bone by ultrasonic bulk and bar velocity measurements. *Clin Rheumatol.* 1999. **18**(1): p. 10-16.
73. Ruegsegger, P., B. Koller, and R. Muller. A microtomographic system for the nondestructive evaluation of bone architecture. *Calcif Tissue Int.* 1996. **58**(1): p. 24-9.

74. Ulrich, D., et al. Finite element analysis of trabecular bone structure: a comparison of image-based meshing techniques. *J Biomech.* 1998. **31**(12): p. 1187-1192.
75. Vaughan, C.L., B.L. Davis, and J.C. O'connor. *Dynamics of human gait.* 1992: Human Kinetics Publishers Champaign, Illinois.
76. Van Rietbergen, B., et al. Trabecular bone tissue strains in the healthy and osteoporotic human femur. *J Bone Miner Res.* 2003. **18**(10): p. 1781-1788.
77. Robinovitch, S., W. Hayes, and T. McMahon. Prediction of femoral impact forces in falls on the hip. *J Biomech Eng.* 1991. **113**(4): p. 366-374.
78. Linde, F., et al. Mechanical properties of trabecular bone - Dependency on strain rate. *J Biomech.* 1991. **24**(9): p. 803-9.
79. Shi, X.T., X. Wang, and G. Niebur. Effects of loading orientation on the morphology of the predicted yielded regions in trabecular bone. *Ann Biomed Eng.* 2009. **37**(2): p. 354-362.
80. Yao, X., et al. Microstructures and properties of cancellous bone of avascular necrosis of femoral heads. *Acta Mechanica Sinica.* 2010. **26**(1): p. 13-19.
81. Teng, S. and S.W. Herring. A stereological study of trabecular architecture in the mandibular condyle of the pig. *Arch Oral Biol.* 1995. **40**(4): p. 299-310.
82. Mulder, L., et al. Biomechanical consequences of developmental changes in trabecular architecture and mineralization of the pig mandibular condyle. *J Biomech.* 2007. **40**(7): p. 1575-1582.
83. Silva, M.J., T.M. Keaveny, and W.C. Hayes. Load sharing between the shell and centrum in the lumbar vertebral body. *Spine (Phila Pa 1976).* 1997. **22**(2): p. 140-50.
84. Liu, X.S., et al. Micromechanical analyses of vertebral trabecular bone based on individual trabeculae segmentation of plates and rods. *J Biomech.* 2009. **42**(3): p. 249-56.
85. Gibson, L.J. Biomechanics of cellular solids. *J Biomech.* 2005. **38**(3): p. 377-399.
86. Gibson, L.J. and M.F. Ashby. *Cellular Solids: Structure and Properties.* 1999: Cambridge University Press.

87. Keaveny, T.M., et al. Differences between the tensile and compressive strengths of bovine tibial trabecular bone depend on modulus. *J Biomech.* 1994. **27**(9): p. 1137-46.
88. Bayraktar, H.H. and T.M. Keaveny. Mechanisms of uniformity of yield strains for trabecular bone. *J Biomech* 2004. **37**(11): p. 1671-1678.
89. Homminga, J., et al. The dependence of the elastic properties of osteoporotic cancellous bone on volume fraction and fabric. *J Biomech* 2003. **36**(10): p. 1461-1467.
90. Kabel, J., et al. Constitutive relationships of fabric, density, and elastic properties in cancellous bone architecture. *Bone.* 1999. **25**(4): p. 481-486.
91. Kabel, J., et al. The role of an effective isotropic tissue modulus in the elastic properties of cancellous bone. *J Biomech* 1999. **32**(7): p. 673-680.
92. Kinney, J.H. and A.J.C. Ladd. The relationship between three-dimensional connectivity and the elastic properties of trabecular bone. *J Bone Miner Res.* 1998. **13**(5): p. 839-845.
93. Ladd, A.J.C., et al. Finite-element modeling of trabecular bone: Comparison with mechanical testing and determination of tissue modulus. *J Orthop Res.* 1998. **16**(5): p. 622-628.
94. Pithioux, M., P. Lasaygues, and P. Chabrand. An alternative ultrasonic method for measuring the elastic properties of cortical bone. *J Biomech.* 2002. **35**(7): p. 961-968.
95. Jørgensen, C.S. and T. Kundu. Measurement of material elastic constants of trabecular bone: A micromechanical analytic study using a 1 GHz acoustic microscope. *J Orthop Res.* 2002. **20**(1): p. 151-158.
96. Nicholson, P.H.F., et al. Structural and material mechanical properties of human vertebral cancellous bone. *Med Eng Phys.* 1997. **19**(8): p. 729-737.
97. Padilla, F., et al. Relationships of trabecular bone structure with quantitative ultrasound parameters: In vitro study on human proximal femur using transmission and backscatter measurements. *Bone.* 2008. **42**(6): p. 1193-1202.

98. Sebaa, N., et al. Application of fractional calculus to ultrasonic wave propagation in human cancellous bone. *Signal Processing*. 2006. **86**(10): p. 2668-2677.
99. Ryan, S.D. and J.L. Williams. Tensile testing of rodlike trabeculae excised from bovine femoral bone. *J Biomech* 1989. **22**(4): p. 351-355.
100. Brouwers, J., et al. Determination of rat vertebral bone compressive fatigue properties in untreated intact rats and zoledronic-acid-treated, ovariectomized rats. *Osteoporosis Int*. 2009. **20**(8): p. 1377-1384.
101. D. R. Carter, W.C.H. The compressive behavior of bone as a two-phase porous structure. *J Bone Joint Surg*. 1977. **59**(7): p. 954-962.
102. Rohlmann, A., et al. Material properties of femoral cancellous bone in axial loading. 1. Time-independent properties. *Arch Orthop Trauma Surg*. 1980. **97**(2): p. 95-102.
103. Mosekilde, L. and C.C. Danielsen. Biomechanical competence of vertebral trabecular bone in relation to ash density and age in normal individuals. *Bone*. 1987. **8**(2): p. 79-86.
104. Ashman, R.B. and R. Jae Young. Elastic modulus of trabecular bone material. *J Biomech* 1988. **21**(3): p. 177-181.
105. Linde, F., I. Hvid, and B. Pongsoipetch. Energy absorptive properties of human trabecular bone specimens during axial compression. *J Orthop Res*. 1989. **7**(3): p. 432-439.
106. Turner, C.H. Yield behavior of bovine cancellous bone. *J Biomech Eng*. 1989. **111**(3): p. 256-260.
107. Lotz, J.C., T.N. Gerhart, and W.C. Hayes. Mechanical-properties of trabecular bone from the proximal femur: A quantitative CT study. *J Comput Assist Tomogr*. 1990. **14**(1): p. 107-114.
108. Ciarelli, M.J., et al. Evaluation of orthogonal mechanical-properties and density of human trabecular bone from the major metaphyseal regions with materials testing and computed-tomography. *J Orthop Res*. 1991. **9**(5): p. 674-682.
109. Rohl, L., et al. Tensile and compressive properties of cancellous bone. *J Biomech* 1991. **24**(12): p. 1143-1149.

110. Keller, T.S. Predicting the compressive mechanical-behavior of bone. *J Biomech* 1994. **27**(9): p. 1159-1168.
111. Keaveny, T.M., et al. Trabecular bone exhibits fully linear elastic behavior and yields at low strains. *J Biomech* 1994. **27**(9): p. 1127-&.
112. Keaveny, T.M., et al. Systematic and random errors in compression testing of trabecular bone *J Orthop Res.* 1999. **17**(1): p. 151-151.
113. Kopperdahl, D.L. and T.M. Keaveny. Yield strain behavior of trabecular bone. *J Biomech* 1998. **31**(7): p. 601-608.
114. Hou, F.J., et al. Human vertebral body apparent and hard tissue stiffness. *J Biomech* 1998. **31**(11): p. 1009-1015.
115. Chang, W.C.W., et al. Uniaxial yield strains for bovine trabecular bone are isotropic and asymmetric. *J Orthop Res.* 1999. **17**(4): p. 582-585.
116. Morgan, E.F. and T.M. Keaveny. Dependence of yield strain of human trabecular bone on anatomic site. *J Biomech* 2001. **34**(5): p. 569-577.
117. Giesen, E.B.W., et al. Mechanical properties of cancellous bone in the human mandibular condyle are anisotropic. *J Biomech* 2001. **34**(6): p. 799-803.
118. Carter, D.R. and W.C. Hayes. The compressive behavior of bone as a two-phase porous structure. *J Bone Joint Surg.* 1977. **59**(7): p. 954-962.
119. Gibson, L.J. The mechanical behaviour of cancellous bone. *J Biomech.* 1985. **18**(5): p. 317-328.
120. Morgan, E.F., H.H. Bayraktar, and T.M. Keaveny. Trabecular bone modulus–density relationships depend on anatomic site. *J Biomech.* 2003. **36**(7): p. 897-904.
121. Morgan, E.F. and T.M. Keaveny. Dependence of yield strain of human trabecular bone on anatomic site. *J Biomech.* 2001. **34**(5): p. 569-577.
122. McCalden, R.W. and J.A. McGeough. Age-Related Changes in the Compressive Strength of Cancellous Bone. The Relative Importance of Changes in Density and Trabecular Architecture. *J Bone Joint Surg.* 1997. **79**(3): p. 421-7.
123. Pugh, J.W., E.L. Radin, and R.M. Rose. Quantitative studies of human subchondral cancellous bone. *J Bone Joint Surg.* 1974. **56**(2): p. 313-321.

124. Hipp, J.A., A.E. Rosenberg, and W.C. Hayes. Mechanical properties of trabecular bone within and adjacent to osseous metastases. *J Bone Miner Res.* 1992. **7**(10): p. 1165-1171.
125. Townsend, P.R., R.M. Rose, and E.L. Radin. Buckling studies of single human trabeculae. *J Biomech.* 1975. **8**(3-4): p. 199-201.
126. Fondrk, M., et al. Some viscoplastic characteristics of bovine and human cortical bone. *J Biomech.* 1988. **21**(8): p. 623-30.
127. Ochoa, J., et al. Stiffening of the femoral head due to intertrabecular fluid and intraosseous pressure. *J Biomech Eng.* 1991. **113**(3): p. 259-262.
128. Linde, F., et al. Mechanical-properties of trabecular bone - dependency on strain rate. *J Biomech.* 1991. **24**(9): p. 803-809.
129. Szabo, M.E., M. Taylor, and P.J. Thurner. Mechanical properties of single bovine trabeculae are unaffected by strain rate. *J Biomech* 2011. **44**(5): p. 962-967.
130. Galante, J., W. Rostoker, and R.D. Ray. Physical properties of trabecular bone. *Calcif Tissue Res.* 1970. **5**(3): p. 236-246.
131. Garo, A., et al. Calibration of the mechanical properties in a finite element model of a lumbar vertebra under dynamic compression up to failure. *Med Biol Eng Comput.* 2011. **49**(12): p. 1371-1379.
132. Keaveny, T.M., E.F. Wachtel, and D.L. Kopperdahl. Mechanical behavior of human trabecular bone after overloading. *J Orthop Res.* 1999. **17**(3): p. 346-353.
133. Kopperdahl, D.L., J.L. Pearlman, and T.M. Keaveny. Biomechanical consequences of an isolated overload on the human vertebral body. *J Orthop Res.* 2000. **18**(5): p. 685-690.
134. Fondrk, M., E. Bahniuk, and D. Davy. A damage model for nonlinear tensile behavior of cortical bone. *J Biomech Eng.* 1999. **121**(5): p. 533-541.
135. Vashishth, D., et al. In vivo diffuse damage in human vertebral trabecular bone. *Bone.* 2000. **26**(2): p. 147-152.
136. Nagaraja, S., T.L. Couse, and R.E. Guldberg. Trabecular bone microdamage and microstructural stresses under uniaxial compression. *J Biomech* 2005. **38**(4): p. 707-716.

137. Tang, S. and D. Vashishth. A non-invasive in vitro technique for the three-dimensional quantification of microdamage in trabecular bone. *Bone*. 2007. **40**(5): p. 1259-1264.
138. Wang, X., et al. Detection of trabecular bone microdamage by micro-computed tomography. *J Biomech*. 2007. **40**(15): p. 3397-3403.
139. Diab, T. and D. Vashishth. Effects of damage morphology on cortical bone fragility. *Bone*. 2005. **37**(1): p. 96-102.
140. Ding, M. and I. Hvid. Quantification of age-related changes in the structure model type and trabecular thickness of human tibial cancellous bone. *Bone*. 2000. **26**(3): p. 291-295.
141. Arlot, M.E., et al. Microarchitecture Influences Microdamage Accumulation in Human Vertebral Trabecular Bone. *J Bone Miner Res*. 2008. **23**(10): p. 1613-1618.
142. Nagaraja, S., A.S. Lin, and R.E. Guldborg. Age-related changes in trabecular bone microdamage initiation. *Bone*. 2007. **40**(4): p. 973-80.
143. Karim, L. and D. Vashishth. Role of trabecular microarchitecture in the formation, accumulation, and morphology of microdamage in human cancellous bone. *J Orthop Res*. 2011. **29**(11): p. 1739-1744.
144. Mughrabi, H., *Cyclic strain localization in fatigued metals*, in *Physical Aspects of Fracture*, E. Bouchaud, et al., Editors. 2001, Springer Netherlands. p. 271-281.
145. Moore, T.L. and L.J. Gibson. Fatigue microdamage in bovine trabecular bone. *J Biomech Eng*. 2003. **125**(6): p. 769-76.
146. Basquin, O. *The exponential law of endurance tests*. in *Proc. ASTM*. 1910.
147. Coffin, L. A note on low cycle fatigue laws (Plastic strain range-fatigue life behavior as two slope relationship, considering low cycle fatigue laws in terms of crack propagation mode change). *J Mater*. 1971. **6**: p. 388-402.
148. Manson, S., *Low cycle fatigue*, in *NASA Technical Note*. 1954, NASA: Lewis Research Center Cleveland, Ohio, USA. p. 2933.
149. King, A. and F. Evans. *Analysis of fatigue strength of human compact bone by the Weibull method*. in *Dig 7th Int. Conf. Med and Biol Eng*. 1967.

150. Carter, D.R., et al. Uniaxial fatigue of human cortical bone. The influence of tissue physical characteristics. *J Biomech* 1981. **14**(7): p. 461-470.
151. Zioupos, P. and A. Casinos. Cumulative damage and the response of human bone in two-step loading fatigue. *J Biomech* 1998. **31**(9): p. 825-833.
152. Yeni, Y.N. and D.P. Fyhrie. Fatigue damage-fracture mechanics interaction in cortical bone. *Bone*. 2002. **30**(3): p. 509-514.
153. O'Brien, F.J., D. Taylor, and T.C. Lee. Microcrack accumulation at different intervals during fatigue testing of compact bone. *J Biomech*. 2003. **36**(7): p. 973-80.
154. Taylor, D., et al. The fatigue strength of compact bone in torsion. *J Biomech* 2003. **36**(8): p. 1103-1109.
155. George, W.T. and D. Vashishth. Susceptibility of aging human bone to mixed-mode fracture increases bone fragility. *Bone*. 2006. **38**(1): p. 105-11.
156. Moore, T.L. and L.J. Gibson. Fatigue of bovine trabecular bone. *J Biomech Eng*. 2003. **125**(6): p. 761-768.
157. Cowin, S.C. The relationship between the elasticity tensor and the fabric tensor. *Mech Mater*. 1985. **4**(2): p. 137-147.
158. Ganguly, P., T.L. Moore, and L.J. Gibson. A phenomenological model for predicting fatigue life in bovine trabecular bone. *J Biomech Eng*. 2004. **126**(3): p. 330-9.
159. Martin, R.B. Fatigue microdamage as an essential element of bone mechanics and biology. *Calcif Tissue Int*. 2003. **73**(2): p. 101-107.
160. Holden, J.P. and P.R. Cavanagh. The free moment of ground reaction in distance running and its changes with pronation. *J Biomech*. 1991. **24**(10): p. 887-97.
161. Pozderac, R.V. Longitudinal tibial fatigue fracture: an uncommon stress fracture with characteristic features. *Clin Nucl Med*. 2002. **27**(7): p. 475-8.
162. Lin, H.C., C.S. Chou, and T.C. Hsu. Stress fractures of the ribs in amateur golf players. *Zhonghua Yi Xue Za Zhi (Taipei)*. 1994. **54**(1): p. 33-7.
163. Williams, T.R., et al. Acetabular stress fractures in military endurance athletes and recruits: incidence and MRI and scintigraphic findings. *Skeletal Radiol*. 2002. **31**(5): p. 277-81.

164. Matheson, G.O., et al. Stress fractures in athletes. A study of 320 cases. *Am J Sports Med.* 1987. **15**(1): p. 46-58.
165. Bowman, S.M., et al. Creep contributes to the fatigue behavior of bovine trabecular bone. *J Biomech Eng.* 1998. **120**(5): p. 647-54.
166. Moore, T.L., F.J. O'Brien, and L.J. Gibson. Creep does not contribute to fatigue in bovine trabecular bone. *J Biomech Eng.* 2004. **126**(3): p. 321-329.
167. Cowin, S.C. Fabric dependence of an anisotropic strength criterion. *Mech Mater.* 1986. **5**(3): p. 251-260.
168. Pietruszczak, S., D. Inglis, and G. Pande. A fabric-dependent fracture criterion for bone. *J Biomech.* 1999. **32**(10): p. 1071-1079.
169. Keaveny, T., et al. Application of the Tsai–Wu quadratic multiaxial failure criterion to bovine trabecular bone. *J Biomech Eng.* 1999. **121**(1): p. 99-107.
170. Fenech, C.M. and T.M. Keaveny. A cellular solid criterion for predicting the axial-shear failure properties of bovine trabecular bone. *J Biomech Eng.* 1999. **121**(4): p. 414-422.
171. Rincón-Kohli, L. and P.K. Zysset. Multi-axial mechanical properties of human trabecular bone. *Biomech Model Mechan.* 2009. **8**(3): p. 195-208.
172. Wolfram, U., et al. Fabric-based Tsai–Wu yield criteria for vertebral trabecular bone in stress and strain space. *J Mech Behav Biomed Mater.* 2012. **15**: p. 218-228.
173. Keaveny, T.M., et al. Application of the Tsai-Wu quadratic multiaxial failure criterion to bovine trabecular bone. *J Biomech Eng.* 1999. **121**(1): p. 99-107.
174. Zysset, P. and L. Rincón, *An alternative fabric-based yield and failure criterion for trabecular bone*, in *Mechanics of Biological Tissue*, G. Holzapfel and R. Ogden, Editors. 2006, Springer Berlin Heidelberg. p. 457-470.
175. Rincón-Kohli, L. and P. Zysset. Multi-axial mechanical properties of human trabecular bone. *Biomech Model Mechan.* 2009. **8**(3): p. 195-208.
176. Keyak, J.H. and S.A. Rossi. Prediction of femoral fracture load using finite element models: an examination of stress-and strain-based failure theories. *J Biomech.* 2000. **33**(2): p. 209-214.

177. Keyak, J. Improved prediction of proximal femoral fracture load using nonlinear finite element models. *Med Eng Phys.* 2001. **23**(3): p. 165-173.
178. Keaveny, T.M., et al. Differences between the tensile and compressive strengths of bovine tibial trabecular bone depend on modulus. *J Biomech.* 1994. **27**(9): p. 1137-1146.
179. Ford, C.M. and T.M. Keaveny. The dependence of shear failure properties of trabecular bone on apparent density and trabecular orientation. *J Biomech.* 1996. **29**(10): p. 1309-1317.
180. Niebur, G.L., M.J. Feldstein, and T.M. Keaveny. Biaxial failure behavior of bovine tibial trabecular bone. *J Biomech Eng.* 2002. **124**(6): p. 699-705.
181. Rowlands, R.E. Strength (failure) theories and their experimental correlation. *Elsevier Science Publishers B. V., Handbook of Composites.* 1985. **3**: p. 71-125.
182. Stone, J.L., G.S. Beaupre, and W.C. Hayes. Multiaxial strength characteristics of trabecular bone. *J Biomech.* 1983. **16**(9): p. 743-52.
183. Fenech, C.M. and T.M. Keaveny. A cellular solid criterion for predicting the axial-shear failure properties of bovine trabecular bone. *J Biomech Eng.* 1999. **121**(4): p. 414-422.
184. Hill, R. A theory of the yielding and plastic flow of anisotropic metals. *Proc Royal Soc Lond A Math Phys Sci.* 1948: p. 281-297.
185. Ottosen, N.S. and M. Ristinmaa. *The mechanics of constitutive modeling.* 2005: Elsevier.
186. Tsai, S.W. and E.M. Wu. A general theory of strength for anisotropic materials. *J Compos Mater.* 1971. **5**(1): p. 58-80.
187. George, W. and D. Vashishth. Influence of phase angle between axial and torsional loadings on fatigue fractures of bone. *J Biomech.* 2005. **38**(4): p. 819-825.
188. Ashby, M.F. and R.M. Medalist. The mechanical properties of cellular solids. *Metal Trans A.* 1983. **14**(9): p. 1755-1769.
189. Chen, P.-Y. and J. McKittrick. Compressive mechanical properties of demineralized and deproteinized cancellous bone. *J Mech Behav Biomed Mater.* 2011. **4**(7): p. 961-973.

190. Cook, R. and P. Zioupos. The fracture toughness of cancellous bone. *J Biomech.* 2009. **42**(13): p. 2054-2060.
191. Cumier, A. Micro-compression: A novel technique for the nondestructive assessment of local bone failure. *Technol Health Care.* 1998. **6**: p. 433-444.
192. Nazarian, A. and R. Müller. Time-lapsed microstructural imaging of bone failure behavior. *J Biomech.* 2004. **37**(1): p. 55-65.
193. Hodgskinson, R. and J. Currey. The effect of variation in structure on the Young's modulus of cancellous bone: A comparison of human and non-human material. *Proc. Inst. Mech. Eng. H.* 1990. **204**(2): p. 115-121.
194. Turner, C.H. and S.C. Cowin. Dependence of elastic constants of an anisotropic porous material upon porosity and fabric. *J Mater Sci.* 1987. **22**(9): p. 3178-3184.
195. Boehler, J.-P. *Applications of tensor functions in solid mechanics.* Vol. 292. 1987: Springer.
196. Zysset, P., R. Goulet, and S. Hollister. A global relationship between trabecular bone morphology and homogenized elastic properties. *J Biomech Eng.* 1998. **120**(5): p. 640-646.
197. Zysset, P.K. A review of morphology–elasticity relationships in human trabecular bone: theories and experiments. *J Biomech.* 2003. **36**(10): p. 1469-1485.
198. Matsuura, M., et al. The role of fabric in the quasi-static compressive mechanical properties of human trabecular bone from various anatomical locations. *Biomech Model Mechan.* 2008. **7**(1): p. 27-42.
199. Silva, M. and L. Gibson. Modeling the mechanical behavior of vertebral trabecular bone: Effects of age-related changes in microstructure. *Bone.* 1997. **21**(2): p. 191-199.
200. Silva, M.J. and L.J. Gibson. The effects of non-periodic microstructure and defects on the compressive strength of two-dimensional cellular solids. *Int J Mech Sci.* 1997. **39**(5): p. 549-563.
201. Yeh, O.C. and T.M. Keaveny. Biomechanical effects of intraspecimen variations in trabecular architecture: A three-dimensional finite element study. *Bone.* 1999. **25**(2): p. 223-228.

202. van Rietbergen, B., et al. A new method to determine trabecular bone elastic properties and loading using micromechanical finite-element models. *J Biomech.* 1995. **28**(1): p. 69-81.
203. Hollister, S.J., J.M. Brennan, and N. Kikuchi. A homogenization sampling procedure for calculating trabecular bone effective stiffness and tissue level stress. *J Biomech* 1994. **27**(4): p. 433-444.
204. Niebur, G.L. and T.M. Keaveny, *Computational modeling of trabecular bone mechanics*, in *Comput Model Biomech.* 2010, Springer. p. 277-306.
205. Shi, X., et al. Type and orientation of yielded trabeculae during overloading of trabecular bone along orthogonal directions. *J Biomech.* 2010. **43**(13): p. 2460-2466.
206. Pauchard, Y., et al. European Society of Biomechanics SM Perren Award 2008: Using temporal trends of 3D bone micro-architecture to predict bone quality. *J Biomech.* 2008. **41**(14): p. 2946-2953.
207. van Rietbergen, B., *Micro-FE analyses of bone: State of the art*, in *Noninvasive assessment of trabecular bone architecture and the competence of bone.* 2001, Springer. p. 21-30.
208. Keaveny, T.M. and D.L. Bartel. Fundamental load transfer patterns for press-fit, surface-treated intramedullary fixation stems. *J Biomech* 1994. **27**(9): p. 1147-1157.
209. Keaveny, T.M. and D.L. Bartel. Effects of porous coating and collar support on early load transfer for a cementless hip prosthesis. *J Biomech* 1993. **26**(10): p. 1205-1216.
210. Augustin, G., et al. Cortical bone drilling and thermal osteonecrosis. *Clin Biomech.* 2012. **27**(4): p. 313-325.
211. Moore, T.A. and L. Gibson. Microdamage accumulation in bovine trabecular bone in uniaxial compression. *J Biomech Eng.* 2002. **124**(1): p. 63-71.
212. Kasra, M. and M.D. Grynbas. On shear properties of trabecular bone under torsional loading: Effects of bone marrow and strain rate. *J Biomech* 2007. **40**(13): p. 2898-2903.

213. Mueller, K.H., A. Trias, and R.D. Ray. *Bone Density and Composition*. Age-related and pathological changes in water and mineral content. Vol. 48. 1966. 140-148.
214. Beaupied, H., E. Lespessailles, and C.-L. Benhamou. Evaluation of macrostructural bone biomechanics. *Joint Bone Spine*. 2007. **74**(3): p. 233-239.
215. Lind, P.M., et al. Torsional testing and peripheral quantitative computed tomography in rat humerus. *Bone*. 2001. **29**(3): p. 265-270.
216. Burgers, T.A., et al. Compressive properties of trabecular bone in the distal femur. *J Biomech* 2008. **41**(5): p. 1077-1085.
217. Bruyere Garnier, K., et al. Mechanical characterization in shear of human femoral cancellous bone: Torsion and shear tests. *Med Eng Phys*. 1999. **21**(9): p. 641-9.
218. Hildebrand, T., et al. Direct Three-Dimensional Morphometric Analysis of Human Cancellous Bone: Microstructural Data from Spine, Femur, Iliac Crest, and Calcaneus. *J Bone Miner Res*. 1999. **14**(7): p. 1167-1174.
219. Gupta, A., et al. Constitutive modeling and algorithmic implementation of a plasticity-like model for trabecular bone structures. *Comput Mech*. 2007. **40**(1): p. 61-72.
220. Dagan, D., M. Be'ery, and A. Gefen. Single-trabecula building block for large-scale finite element models of cancellous bone. *Mech Biol Eng Comput*. 2004. **42**(4): p. 549-556.
221. Burla, R.K., A.V. Kumar, and B.V. Sankar. Implicit boundary method for determination of effective properties of composite microstructures. *Int J Solids Struct*. 2009. **46**(11-12): p. 2514-2526.
222. Bartoska, R. Measurement of femoral head diameter: A clinical study. *Acta Chir Orthop Traumatol Cech*. 2009. **76**(2): p. 133-6.
223. Garcia, D., et al. A three-dimensional elastic plastic damage constitutive law for bone tissue. *Biomech Model Mechan*. 2009. **8**(2): p. 149-165.
224. Bright, J.A. and E.J. Rayfield. Sensitivity and ex vivo validation of finite element models of the domestic pig cranium. *J Anat*. 2011. **219**(4): p. 456-471.

225. Strait, D.S., et al. Modeling elastic properties in finite-element analysis: How much precision is needed to produce an accurate model? *Anat Rec A Discov Mol Cell Evol Biol.* 2005. **283A**(2): p. 275-287.
226. Bourne, B.C. and M.C. van der Meulen. Finite element models predict cancellous apparent modulus when tissue modulus is scaled from specimen CT-attenuation. *J Biomech.* 2004. **37**(5): p. 613-21.
227. Ashman, R.B., J.D. Corin, and C.H. Turner. Elastic properties of cancellous bone: Measurement by an ultrasonic technique. *J Biomech* 1987. **20**(10): p. 979-986.
228. Wang, X., et al. Axial-shear interaction effects on microdamage in bovine tibial trabecular bone. *Eur J Morphol.* 2005. **42**(1/2): p. 61-70.
229. Goldstein, S.A., et al. The mechanical properties of human tibial trabecular bone as a function of metaphyseal location. *J Biomech.* 1983. **16**(12): p. 965-969.
230. Kaplan, S.J., et al. Tensile strength of bovine trabecular bone. *J Biomech.* 1985. **18**(9): p. 723-727.
231. Williams, J. and J. Lewis. Properties and an anisotropic model of cancellous bone from the proximal tibial epiphysis. *J Biomech Eng.* 1982. **104**(1): p. 50-56.
232. Halawa, M., et al. The shear strength of trabecular bone from the femur, and some factors affecting the shear strength of the cement-bone interface. *Arch Orthop Trauma Surg.* 1978. **92**(1): p. 19-30.
233. Vale, A.C., et al. Effect of the strain rate on the twisting of trabecular bone from women with hip fracture. *J Biomech Eng.* 2013. **135**(12): p. 121005.
234. Borchers, R.E., et al. Effects of selected thermal variables on the mechanical properties of trabecular bone. *Biomaterials.* 1995. **16**(7): p. 545-551.
235. Cory, E., et al. Compressive axial mechanical properties of rat bone as functions of bone volume fraction, apparent density and micro-CT based mineral density. *J Biomech.* 2010. **43**(5): p. 953-60.
236. Mitton, D., et al. The effects of density and test conditions on measured compression and shear strength of cancellous bone from the lumbar vertebrae of ewes. *Med Eng Phys.* 1997. **19**(5): p. 464-74.

237. Robertson, D.M. and D.C. Smith. Compressive strength of mandibular bone as a function of microstructure and strain rate. *J Biomech* 1978. **11**(10–12): p. 455-471.
238. Saha, S., Gorman, P. H. Strength of human cancellous bone in shear and its relationship to bone mineral content. *Trans Orthop Res*. 1981: p. 217.
239. Syahrom, A., et al. Mechanical and microarchitectural analyses of cancellous bone through experiment and computer simulation. *Med Biol Eng Comput*. 2011. **49**(12): p. 1393-1403.
240. Guillen, T., et al. Compressive behaviour of bovine cancellous bone and bone analogous materials, microCT characterisation and FE analysis. *J Mech Behav Biomed Mater* 2011. **4**(7): p. 1452-1461.
241. Niebur, G.L., M.J. Feldstein, and T.M. Keaveny. Biaxial Failure Behavior of Bovine Tibial Trabecular Bone. *J Biomech Eng*. 2002. **124**(6): p. 699.
242. Lotz, J.C., E.J. Cheal, and W.C. Hayes. Fracture prediction for the proximal femur using finite element models: Part II-nonlinear analysis. *J Biomech Eng*. 1991. **113**(4): p. 361-5.
243. Cheal, E.J., et al. Stress analysis of a condylar knee tibial component: influence of metaphyseal shell properties and cement injection depth. *J Orthop Res*. 1985. **3**(4): p. 424-434.
244. Wang, X. and G.L. Niebur. Microdamage propagation in trabecular bone due to changes in loading mode. *J Biomech*. 2006. **39**(5): p. 781-790.
245. Niebur, G.L., M.J. Feldstein, and T.M. Keaveny. Biaxial failure behavior of bovine tibial trabecular bone. *J Biomech Eng*. 2002. **124**(6): p. 699-705.
246. Fatihhi, S.J., et al. Uniaxial and Multiaxial Fatigue Life Prediction of the Trabecular Bone Based on Physiological Loading: A Comparative Study. *Ann Biomed Eng*. 2015: p. 1-16.
247. Bergmann, G., F. Graichen, and A. Rohlmann. Hip joint contact forces during stumbling. *Langenbecks Arch Surg*. 2004. **389**(1): p. 53-9.
248. Bergmann, G., et al. Realistic loads for testing hip implants. *Bio-med Mater Eng*. 2010. **20**(2): p. 65-75.
249. Moore, T., F. O'Brien, and L. Gibson. Creep does not contribute to fatigue in bovine trabecular bone. *J Biomech Eng*. 2004. **126**(3): p. 321-329.

250. Smith, J.O. The effect of range of stress on the fatigue strength of metals. *University of Illinois bulletin; vol. 39, no. 26.* 1942.
251. Sines, G. Behavior of metals under complex static and alternating stresses. *Metal Fatigue.* 1959. **1**: p. 145-169.
252. Davoli, P., et al. Independence of the torsional fatigue limit upon a mean shear stress. *Int J Fatigue.* 2003. **25**(6): p. 471-480.
253. Gibson, L.J. Mechanical behavior of metallic foams. *Annu Rev Mater Sci.* 2000. **30**(1): p. 191-227.
254. Burr, D.B., et al. Does microdamage accumulation affect the mechanical properties of bone? *J Biomech.* 1998. **31**(4): p. 337-345.
255. Kummari, S., et al. Trabecular microfracture precedes cortical shell failure in the rat caudal vertebra under cyclic overloading. *Calc Tissue Int.* 2009. **85**(2): p. 127-133.
256. Hoshaw, S., et al. Decrease in canine proximal femoral ultimate strength and stiffness due to fatigue damage. *J Biomech.* 1997. **30**(4): p. 323-329.
257. Wu, Z., A.J. LaNeve, and G.L. Niebur. In vivo microdamage is an indicator of susceptibility to initiation and propagation of microdamage in human femoral trabecular bone. *Bone.* 2013. **55**(1): p. 208-215.
258. Fantner, G.E., et al. Influence of the degradation of the organic matrix on the microscopic fracture behavior of trabecular bone. *Bone.* 2004. **35**(5): p. 1013-1022.
259. Snyder, B., et al. Role of trabecular morphology in the etiology of age-related vertebral fractures. *Calc Tissue Int.* 1993. **53**(1): p. S14-S22.
260. Van Rietbergen, B., et al. Relationships between bone morphology and bone elastic properties can be accurately quantified using high-resolution computer reconstructions. *J Orthop Res.* 1998. **16**(1): p. 23-28.
261. Harrison, N.M., et al. Heterogeneous linear elastic trabecular bone modelling using micro-CT attenuation data and experimentally measured heterogeneous tissue properties. *J Biomech* 2008. **41**(11): p. 2589-2596.
262. Hsieh, Y.F. and M.J. Silva. In vivo fatigue loading of the rat ulna induces both bone formation and resorption and leads to time-related changes in bone mechanical properties and density. *J Orthop Res.* 2002. **20**(4): p. 764-71.

263. Chawla, K.K. *Composite Materials: Science and Engineering*. 2013: Springer New York.
264. Thomsen, J.S., E.N. Ebbesen, and L.i. Mosekilde. Age-related differences between thinning of horizontal and vertical trabeculae in human lumbar bone as assessed by a new computerized method. *Bone*. 2002. **31**(1): p. 136-142.